



Equatorial storm surge risks revealed by the 2001 tropical cyclone Vamei

Masashi Watanabe^{1,2}, Adam D. Switzer^{2,3}, Erandani Lakshani Widana Arachchige², Constance Ting Chua^{2,4}, Jun Yu Puah³, Elaine Tan³, Timothy A. Shaw², David Lallemant²

- ⁵ School of Ocean and Earth Science, University of Southampton, European Way, Southampton, SO14 3ZH, UK
 - ² Earth Observatory of Singapore, Nanyang Technological University, N2-01A-15, 50 Nanyang Avenue, 639798, Singapore
 - ³ Asian School of the Environment, Nanyang Technological University, 50 Nanyang Drive, 639798, Singapore
 - ⁴ Tohoku University, International Research Institute of Disaster Science, 468-1 Aoba Aramaki, Aoba, Sendai, 980-8572, Japan
- 10 Correspondence to: Masashi Watanabe (masashi.watanabe@soton.ac.uk)

Abstract. Tropical Cyclone Vamei, which emerged at 1.5° N on December 27, 2001, challenged the prevailing idea that near-equatorial areas are safe from storm surges, as it resulted in localised flooding in Singapore and Malaysia, revealing a rare yet critical regional hazard. Thus, we investigated storm surge risk assessment in Singapore based on numerical simulations using Delft3D in multiple scenarios. We first validated the accuracy of our simulation results by comparing them with nine observation points around Singapore Island. We then conducted the simulations as a suite of alternative scenarios created by moving the known track of Tropical Cyclone Vamei, modelling more intense storms corresponding to a 1-in-1000-year scenario and considering future sea level rise induced by global warming. When a 1000-year probability of occurrence was assumed, the maximum storm surge height around Singapore increased to 0.595 m. For a 1000-year cyclone with its path shifted 0.8° southward, sea level rise scenarios of +0.7 m and +2.0 m resulted in inundation areas of 34.5 km² and 90.7 km², respectively. While the calculated storm surge height remained largely unchanged despite future sea level rise, the inundation area in Singapore expanded significantly. This indicates that sea level rise is a primary contributor to this expansion, highlighting the importance of considering future sea levels in inundation assessments. Further research is necessary to assess potential changes in the frequency and intensity of tropical cyclones impacting Singapore under future climate scenarios.

25 1 Introduction

Storm surges induced by tropical cyclones have threatened coastal communities worldwide (Dasgupta et al., 2011) and can induce severe economic losses; for example, Neumann et al. (2015) estimated that asset losses due to storm surges and rising sea levels in the USA could reach \$990 billion by 2100. Therefore, investigating storm surge hazards is a critical issue for coastal regions. The coasts in Southeast Asia, including Singapore, have the potential risk of severe surge hazards. Indeed, eight out of the ten most densely populated metropolitan areas around the world are at risk from storm surges in Southeast Asia (SwissRe, 2017).





Tropical cyclones are rarely observed within 5 degrees of the equator (e.g., Gray, 1968; Anthes, 1982; McBride, 1995; Chang et al., 2003) because the Coriolis effect is minimal in these latitudes. This implies that the risk of tropical cyclones and storm surges near the equator is likely negligible. However, this assumption was challenged by Tropical Cyclone Vamei, which formed offshore of western Borneo, southeast of Singapore, on December 27, 2001. This event marked the first recorded tropical cyclone formation within 1.5° of the equator (Chang et al., 2003). The unique formation of tropical cyclone Vamei has since been the subject of several simulation studies (e.g., Chambers and Li, 2007; Juneng et al., 2010; Yi and Zhang, 2010). Chang et al. (2003) estimated its return period to be a rare 100–400 years. Given the extreme rarity of such an event, a thorough understanding of the factors contributing to tropical cyclone formation and the associated storm surge risks in this equatorial region is critically needed. Despite this, the specific risk of storm surge from a tropical cyclone in this particular region still needs to be investigated.

Downward counterfactual analysis is an analytical approach that evaluates the potential outcomes of alternative scenarios by comparing them to a historical event (Woo, 2016; 2019). In storm surge risk analysis, this method allows researchers to examine scenarios such as varying the intensity or path of a tropical cyclone, modifying protective measures like seawalls or drainage systems, or even considering land reclamation projects that alter the coastal landscape. Comparing such scenarios to a historical event makes it possible to assess the relative risk posed by different outcomes. This approach was previously applied to Tropical Cyclone Vamei by Lin et al. (2020), who investigated the consequences of a downward track shift resulting in a direct landfall on Singapore. However, their analysis centered on wind-related impacts, leaving the potential for coastal inundation from storm surge unquantified.

Building upon their work, we investigated the storm surge hazard around Singapore through numerical simulations in multiple scenarios, focusing on Tropical Cyclone Vamei.

55 2 Study area

Singapore, located at 1.290270° N latitude, and 103.851959° E longitude, is a low-lying, maritime city-state with approximately 5.7 million inhabitants (Fig. 1). Land use and land-cover changes in the past century have been transformed by industrialisation and urbanisation processes (Wang et al., 2015). Especially between the 1970s and the 1990s, the transformation was most dramatic because of the rapid expansion of built-up areas for residential estates, industrial and commercial use, and transportation infrastructure in the southeast and southwest of Singapore (Fong et al., 2020). The port and maritime industry in Singapore is valued at about 20 billion USD (accounting for 7 % of its total gross domestic product) and has an annual throughput of 140,000 vessels transporting 33.9 million containers (Maritime and Port Authority of Singapore, 2014). Its landscape consists of one main island, located at the southern tip of the Malay Peninsula, and approximately 45 smaller offshore islands (Tun, 2012). The Singapore Strait, south of Singapore, is one of the busiest





shipping routes in the world (Chen et al., 2005; Tkalich et al., 2013). The tidal currents in the Strait are also greatly affected by the northeast monsoon (Chen et al., 2005). Recent observations have further demonstrated that both tidal forcing and monsoonal winds strongly influence the nonstationary behaviour of coastal currents offshore Singapore (Puah et al., 2024).

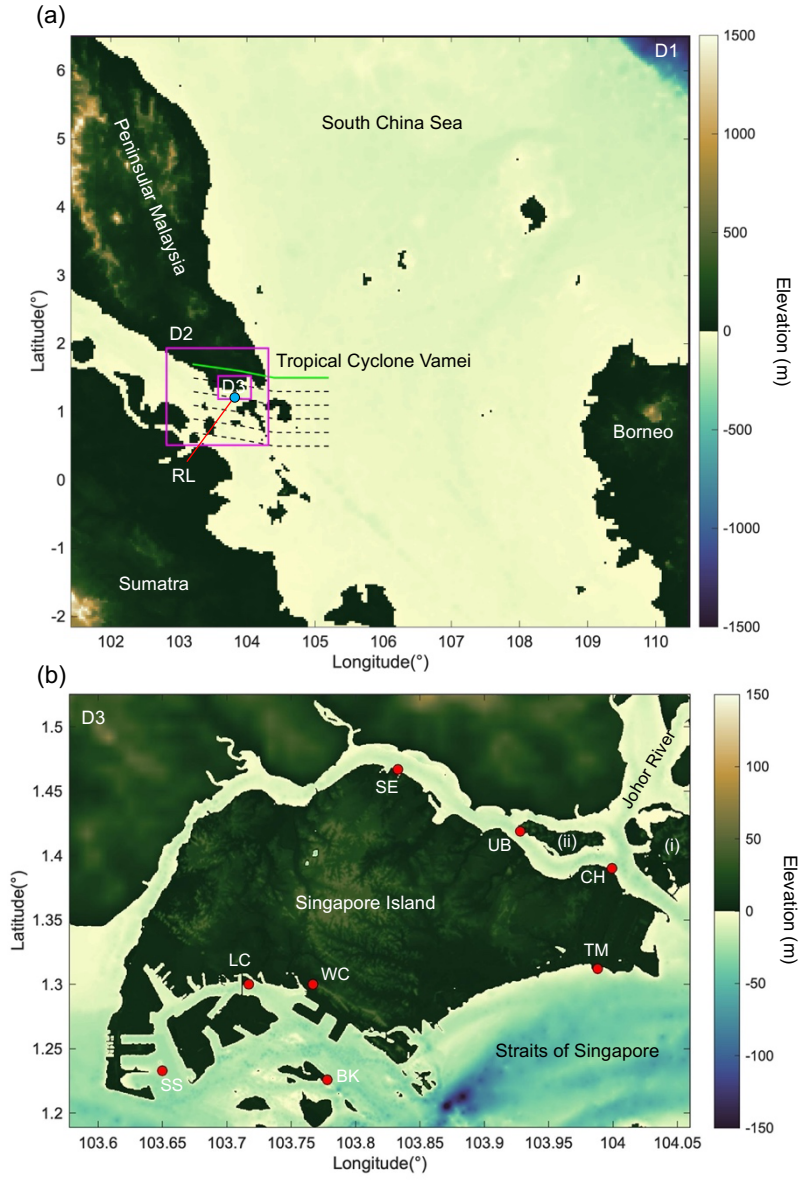


Figure 1: Location of our study area. (a) D1-D3 shown in the figures indicate the computational domains 1-3. The location of the observation points of the water level at RL is also shown. The green line is the actual path of Tropical Cyclone Vamei, reported by JMA, and the dashed black lines are the tropical cyclone paths when the path moves southward from the path of Tropical Cyclone Vamei with an interval of -0.2 degrees. (b) Numerical computational domain in D3. Locations of observation points of the tide that are Bukum (BK), Raffles Light house (RL), Ubin (UB), Tanjong Changi (CH), Sultan Shoal (SS), Tanah Merah (TM), Jurong (LC), Sembawang (SE), and West Coast (WC) are shown. (i) and (ii) are Tekong Island and Pulau Ubin.

https://doi.org/10.5194/egusphere-2025-5703 Preprint. Discussion started: 25 November 2025

© Author(s) 2025. CC BY 4.0 License.





75 3 Data and Methods

Computational modelling of impact scenarios is crucial in understanding the potential consequences of extreme weather events (Tadesse et al., 2020). This study applies Delft3D, a modelling framework widely used to simulate storm surges (Deltares 2011).

Therefore, this section describes the methodology and the data requirements for modelling, the development process using Delft3D, and the presentation of results to enhance the understanding of storm surge hazards.

3.1 Storm surge simulation during Tropical Cyclone Vamei

Delft3D/SWAN (Deltares, 2011) was used to calculate the wave and current fields using the same schemes as Watanabe et al. (2017, 2018). We applied Delft3D, with one vertical layer, which implements the shallow water equations to calculate water elevation and current fields, then passes the numerical result to SWAN (Deltares, 2011). SWAN calculates spectral parameters of the wave field via the conservation of wave action. Then, SWAN passes the numerical result for radiation stresses back to Delft3D so that wave setup and current field induced by wave setup are calculated.

We conducted domain decomposition to output our simulation results around Singapore with fine computational grids. The model resolution was 0.018° for domain D1, 0.0028° for D2, and 0.00048° for D3 (Fig. 1a, and b). Hasan et al. (2016) revealed that a finer resolution of numerical grid cells is needed to reproduce the current tidal situation around Singapore because headlands and small islands influence the bathymetry. Therefore, we conducted domain decomposition and adopted a finer resolution around Singapore in D3. We output simulation results in D3 to reveal storm surge hazards in Singapore. High-resolution bathymetry and elevation data are required to capture the subtle variations in terrain that affect the precise representation of flood-prone areas during storm surge events. For the simulation, we set Manning's roughness coefficients as 0.025 m-1/3 s over beaches, seafloor, and artificial objects such as paved surfaces, following Kotani et al. (1998).

The track of Tropical Cyclone Vamei was observed by the Japan Meteorological Agency (JMA) and the Joint Typhoon Warning Center (JTWC) best-track datasets, which are both included in the IBTrACS (International Best-Track Archive for Climate Stewardship) version 4 dataset (Knapp et al., 2010; Knapp et al., 2018). Observations by JMA showed the maximum wind speed was 45 kt (10-minute mean wind speed), the minimum central pressure was 1006 hPa, and the duration of the tropical cyclone was 18 hours. While observations by the JTWC showed that the maximum wind speed was 65 kt (1-minute mean wind speed), the minimum central pressure was 1008 hPa, and the tropical cyclone's duration was 12 hours (Table 1). Although the cyclone was short-lived, its impact was devastating, unleashing significant flooding and





mudslides in the Johor and Pahang states of Malaysia, which border Singapore to the north, resulting in the evacuation of over 17,000 people and reports of five deaths (Johnson and Chang, 2007).

The data on the behaviour of Tropical Cyclone Vamei used in this calculation were created following Bricker et al. (2014). 110 The observed tropical cyclone path and the central pressure of the tropical cyclone were input into the parametric hurricane model of Holland (1980) to estimate air pressure and wind fields (Fig. 2). To account for these fields' asymmetry due to the tropical cyclone's forward motion, the method was modified following Fujii and Mitsuda (1986). The radius to maximum winds was estimated using the empirical relation of Quiring et al. (2011). Tides are included using the Global Tide database TPXO (TPXO, 2014) as a boundary condition of the first domain in the hydrodynamic model. Before the simulation, we calibrated the tidal current's input time series to reproduce the water level time series at tide gauge points (see Appendix 1). 115 Topography and bathymetry were obtained from GEBCO (IOC et al., 2003) and SRTM data (NASA, 2014). Around Singapore, we used the data from Hydrographic and Nautical Charts (Navionics, 2023), a 10 m Digital Terrain Model (DTM) model from Singapore Land Authority (SLA), GEBCO (IOC et al., 2003), Malaysia land boundaries (Hijman and University of California, 2015), Indonesia land boundaries (Humanitarian Data Exchange, undated), Singapore boundaries 120 (Urban Redevelopment Authority, 2019). The calculation time is three days, from 24 to 27 December 2001. The tide calculation was spun up for three days from 24 to 27 December. From 0:00 on 27 December, the wind and pressure fields were added to the input to calculate storm surges and waves. We conducted the two simulations using tropical cyclone speed, minimum central pressure, and tropical cyclone path observed by JMA and JTWC (Table 1).

When the track observed by JMA was used, we set the simulation from 0:00 to 18:00 in January. When the track observed by JTWC was used, we set the simulation from 0:00 to 12:00 January. The simulation durations were set to match the respective observation periods of the tropical cyclone as recorded by the JMA and the JTWC. Tide gauge data are corrected at nine observational points, including Bukum (BK), Raffles Light house (RL), Ubin (UB), Tanjong Changi (CH), Sultan Shoal (SS), Tanah Merah (TM), Jurong (LC), Sembawang (SE), and West Coast (WC) (Fig. 1b). We compared the calculated maximum water level and observed ones by MPA (personal communication) to validate our simulation results.





JMA

Year. Month. Day. Hour (h)	Latitude (Deg)	Longtitude (Deg)	Central Pressure (hPa)	Wind speed (kt)
2001.12.27.00	1.5	105.2	1008	40
2001.12.27.06	1.5	104.4	1006	45
2001.12.27.12	1.6	103.9	1008	35
2001.12.27.18	1.7	103.2	1010	-
JTWC				
Year. Month. Day. Hour (h)	Latitude (Deg)	Longtitude (Deg)	Central Pressure (hPa)	Wind speed (kt)
2001.12.27.00	1.5	105.1	1008	65
2001.12.27.06	1.5	104.4	1008	65
2001.12.27.12	1.6	103.7	1008	45

Table 2: The paths, central pressures, and wind speeds of the tropical cyclone Vamei reported by JMA and JTWC.

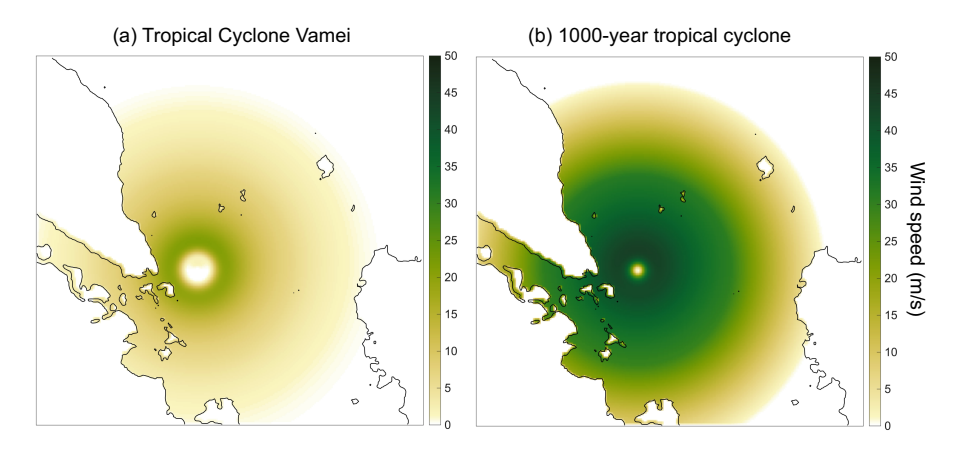


Figure 2: Distribution of wind fields generated using the Holland (2010) model for 0:00 on 27 December. (a) The wind field assuming the actual parameters of Tropical Cyclone Vamei. (b) The wind field assuming a hypothetical Category 2 tropical cyclone with a 1000-year return period.

3.2 Defining the design tropical cyclone: Intensity and Size

We also ran scenarios based on an increase in the typhoon's intensity. We achieved this by considering the return period using the generalised Pareto distribution (GPD). The generalised Pareto distribution (GPD) (e.g., Coles 2001; McInnes et al. 2016) was employed for the typhoon intensity.

$$F(y) = 1 - \left(\frac{1 + \xi(y - u)}{\sigma}\right)^{-\frac{1}{\xi}},\tag{1}$$

https://doi.org/10.5194/egusphere-2025-5703 Preprint. Discussion started: 25 November 2025

© Author(s) 2025. CC BY 4.0 License.



150

155

160

170



where ξ and σ are the shape and scale parameters, and u is the threshold.

In this study, we set *u* as the threshold representing the maximum wind speed and *y* as the maximum wind speed. The parameters in Equation (1) were estimated using the L-Moments method proposed by Hosking (1990). For this estimation, we obtained the observed tropical cyclone data from the Northern Pacific during 2001–2025, published by the JMA. Once the maximum wind speed for a given return period was estimated, the corresponding minimum central pressure was determined using an empirical wind-pressure relationship (WPR) that we developed from the regional JMA dataset. Subsequently, the typhoon's size was defined by calculating the radius of maximum winds (RMW) using the empirical model proposed by Quiring et al. (2011). Finally, we estimated the maximum storm surge around Singapore for scenarios with assumed 1000-year return period tropical cyclones.

We assumed the maximum wind speed is 45 knots, which is the maximum observed wind speed of 45 knots by JMA (Table 1). This is because the calculated storm wave heights were consistent with the observation values when the JMA dataset was used as described in Section 4.1. We collected JMA datasets on the typhoon's date and time, minimum central pressure, and maximum wind speed when it exceeded 45 knots. We employed observational tropical cyclone data from a geographically and climatically relevant sub-region of the western North Pacific, specifically defined as 0-15°N latitude and 100-125°E longitude (southern South China Sea).

This targeted selection is based on several key considerations. First, we excluded data from higher latitudes to mitigate potential biases, as previous studies indicate that cyclone activity varies significantly between regions above and below 20°N in the western North Pacific, particularly in terms of seasonality and trends (Wang et al., 2025; Widana et al., 2025). Second, the chosen domain is close to Singapore and exhibits similar large-scale atmospheric and oceanic conditions that are crucial for the formation of tropical cyclones capable of impacting equatorial areas. Notably, the tropical cyclone climatology of the South China Sea is influenced by monsoon-driven variations in large-scale parameters. For instance, cyclones in the northern South China Sea peak from July to September, while those in the southern region (below 15°N) peak from October to December. Thus, our chosen sub-region (0-15°N latitude and 100-125°E longitude) effectively captures the climatology of tropical cyclones that typically occur from October to December, aligning directly with the occurrence of Typhoon Vamei in December.

We then estimated the cumulative probability of the maximum wind speed of the cyclones using equation (1). From the estimated cumulative probability, we calculated the annual cumulative probability versus the maximum wind speed of the typhoon. The estimated return period of Tropical Cyclone Vamei was 100–400 years (Chang et al., 2003), so we assumed that the return period of Tropical Cyclone Vamei was 250 years. This assumption was used to constrain the model



180

185

190

195

200

205

210



parameters. Specifically, the threshold u in equation (1) is 45 knots, calibrating the model to yield a 250-year return period for the observed intensity of Tropical Cyclone Vamei.

3.3 Simulation cases

The downward counterfactual approach allows researchers to analyse storm surge risks by simulating alternative scenarios based on historical events (Woo, 2016, 2019; Lin et al., 2020). We applied the downward counterfactual approach to determine the worst-case scenario of storm surge events around Singapore. This approach aids in understanding the influence of factors such as storm characteristics, protective measures, and environmental changes on storm surge risks. In this context, using Delft3D, a versatile modelling framework, holds immense potential for simulating storm surges and informing risk management strategies. In this case, the downward counterfactual approach simulates alternative storm scenarios by modifying parameters such as storm intensity, size, translation speed and path within the Delft3D model. By comparing the results of these simulations with the Vamei event in 2001, we have regionally validated a metric-based assessment of the relative storm surge risk associated with different scenarios. Our approach also identifies critical factors contributing to storm surge risks and provides valuable insights for risk management strategies.

We assumed that the end-of-search criteria of the downward counterfactual approach are cases where maximum storm surge is generated around Singapore. If the tropical cyclone's path moves southward, the strong wind speed of the tropical cyclone is expected to strike Singapore (Fig. 1a). Tropical Cyclone Vamei is classified as a Category 1 cyclone (Chen et al., 2005). Thus, this study models a hypothetical intensified scenario in which Vamei reaches 1000-year intensity. According to the projection by CCRS (undated), the mean sea level rise around Singapore will be 0.23 m to 1.15 m by 2099 and around 2.0 m by 2150 under the high emissions scenario. Therefore, we assumed the sea level rises by 2099 and 2015 as 0.7 m and 2.0 m, respectively, and these are also incorporated in our simulation.

In this study, we conducted 20 simulations by changing the intensity and path of the tropical cyclones and future sea level rises (Table 2). When Tropical Cyclone Vamei occurred, the maximum observed tidal water level was 0.92 m. Therefore, all simulations for Cases 1–20 were conducted under this high-tide condition. We moved the path of Tropical cyclone Vamei - 0.2°, -0.4°, -0.6°, -0.8°, and -1.0° southward (Cases 2-6). We also conducted the simulation when a 1000-year tropical cyclone was assumed (Cases 7-12). As we explained in Section 4.4, when the tropical cyclone path was shifted 0.8° southward, the maximum inundation area in Singapore was maximum when the sizes of the actual tropical cyclone Vamei and the 1000-year tropical cyclone were assumed (Table 2). To assess the effects of sea level rise on storm surge, simulations were conducted under two sea level rise scenarios: +0.7 m and +2.0 m (Table 2). For each scenario, four cases were considered. In the +0.7 m sea level rise condition, Case 13 assumed both the path and intensity of Tropical Cyclone Vamei; Case 14 assumed the same intensity as Vamei but with the cyclone path shifted 0.8° southward; Case 15 assumed the





same path as Vamei but with the intensity corresponding to a 1000-year tropical cyclone; and Case 16 assumed both a 0.8° southward-shifted path and the intensity of a 1000-year tropical cyclone. Similarly, under the +2.0 m sea level rise condition, Cases 17 to 20 were defined with the same respective settings as Cases 13 to 16.

Cases	Typhoon path	Typhoon size	Sea level rise	Maximum storm surge height around Singapore (m)	Inundation area (km²)
Case 1	Typhoon Vamei	Typhoon Vamei	+0 m	0.127	8.06
Case 2	0.2° south of actual path	Typhoon Vamei	+0 m	0.172	8.38
Case 3	0.4° south of actual path	Typhoon Vamei	+0 m	0.173	8.53
Case 4	0.6° south of actual path	Typhoon Vamei	+0 m	0.160	8.72
Case 5	0.8° south of actual path	Typhoon Vamei	+0 m	0.173	8.83
Case 6	1.0° south of actual path	Typhoon Vamei	+0 m	0.183	8.62
Case 7	Typhoon Vamei	1000-year probability	+0 m	0.595	10.1
Case 8	0.2° south of actual path	1000-year probability	+0 m	1.08	13.1
Case 9	0.4° south of actual path	1000-year probability	+0 m	1.16	18.1
Case 10	0.6° south of actual path	1000-year probability	+0 m	1.07	20.9
Case 11	0.8° south of actual path	1000-year probability	+0 m	1.21	21.2
Case 12	1.0° south of actual path	1000-year probability	+0 m	1.34	20.7
Case 13	Typhoon Vamei	Typhoon Vamei	+0.7 m	0.135	18.1
Case 14	0.8° south of actual path	Typhoon Vamei	+0.7 m	0.167	19.9
Case 15	Typhoon Vamei	1000-year probability	+0.7 m	0.578	21.8
Case 16	0.8° south of actual path	1000-year probability	+0.7 m	1.24	34.5
Case 17	Typhoon Vamei	Typhoon Vamei	+2.0 m	0.133	51.2
Case 18	0.8° south of actual path	Typhoon Vamei	+2.0 m	0.169	54.1
Case 19	Typhoon Vamei	1000-year probability	+2.0 m	0.503	55.9
Case 20	0.8° south of actual path	1000-year probability	+2.0 m	1.20	90.7

Table 2: Studied cases and assumptions. The calculated maximum storm surge heights in Domain 3 (D3) and the calculated inundation area in Singapore are also shown.

4 Results

215

4.1 The accuracy of the simulation results

First, we compared the maximum water level during the time that Tropical Cyclone Vamei was sustained (Fig. 3, Table 3). From both simulation and observation results, we extracted the maximum water level rise from water levels that the tidal current includes by applying a high-pass filter. In observation and our simulation, the highest and second-highest water level rises by storm surge were recorded at SE and UB, respectively, and the observed storm surge heights at these points are 0.15 and 0.11 m, respectively (Table 3, Fig. 3). This is because these points are located in northern Singapore, close to the tropical cyclone's position. Thus, high storm surges were produced by higher wind velocity and lower pressure. When the tropical



235

240



cyclone track, maximum wind speed, and minimum central pressure observed by JMA were used for the simulation, maximum water levels were underestimated (Table 3, Fig. 3). Meanwhile, when the data observed by JTWC were used, the maximum water levels were overestimated. Thus, the simulation accuracy depended on the accuracy of observation of the tropical cyclone's track, minimum central pressure, and maximum wind speed. We compared the calculated time series of water levels and observed ones at tide gauge points (Fig. 4). The calculated water levels are generally consistent with the observed ones. The inconsistency of the time series of water levels is due to the accuracy of the tide simulation model. This is because the input water levels of the tide are from TPXO data, which is interpolated from observed tidal data (TPXO, 2014) and was used for this simulation. If we input the observed time series of the tide or calculate the tidal current on a global scale, the simulation accuracy of the tidal current increases. However, this study focuses on storm surges around Singapore, and the accuracy of storm surge simulation was validated by comparing simulation results with observation results (Table 3, Fig. 4). Therefore, improving the simulation accuracy of tidal currents is beyond the scope of this study.

	Observed	Calculated (JMA)	Calculated (JTWC)
RL	0.064	0.050	0.046
BK	0.066	0.050	0.088
СН	0.075	0.039	0.18
LC	0.071	0.049	0.15
SE	0.15	0.093	0.30
SS	0.050	0.057	0.070
TM	0.069	0.042	0.090
UB	0.11	0.072	0.30
WC	0.084	0.050	0.14

Table 3: Observed and calculated maximum water levels at BK, RL, UB, CH, SS, TM, LC, SE, and WC. The locations of observation points are indicated in Fig. 1. The two calculation results using tropical cyclone paths, central pressure, and wind speed reported by JMA and JTWC are shown.





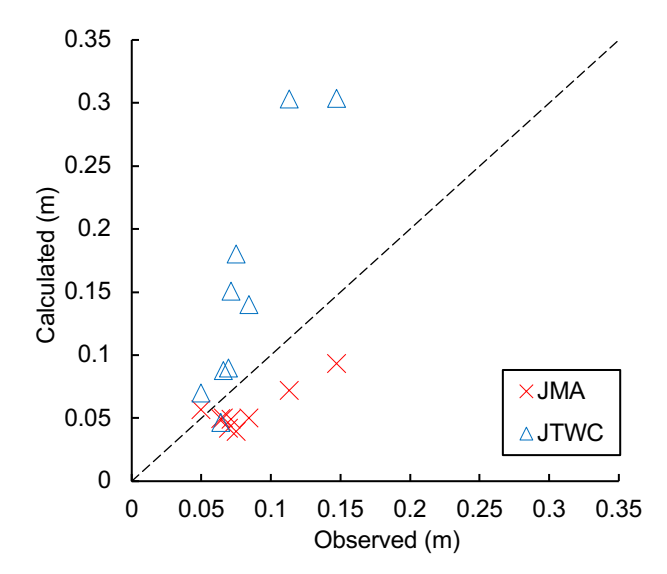


Figure 3: Observed versus calculated peak water levels (m) using storm parameters from JMA (red crosses) and JTWC (blue triangles).





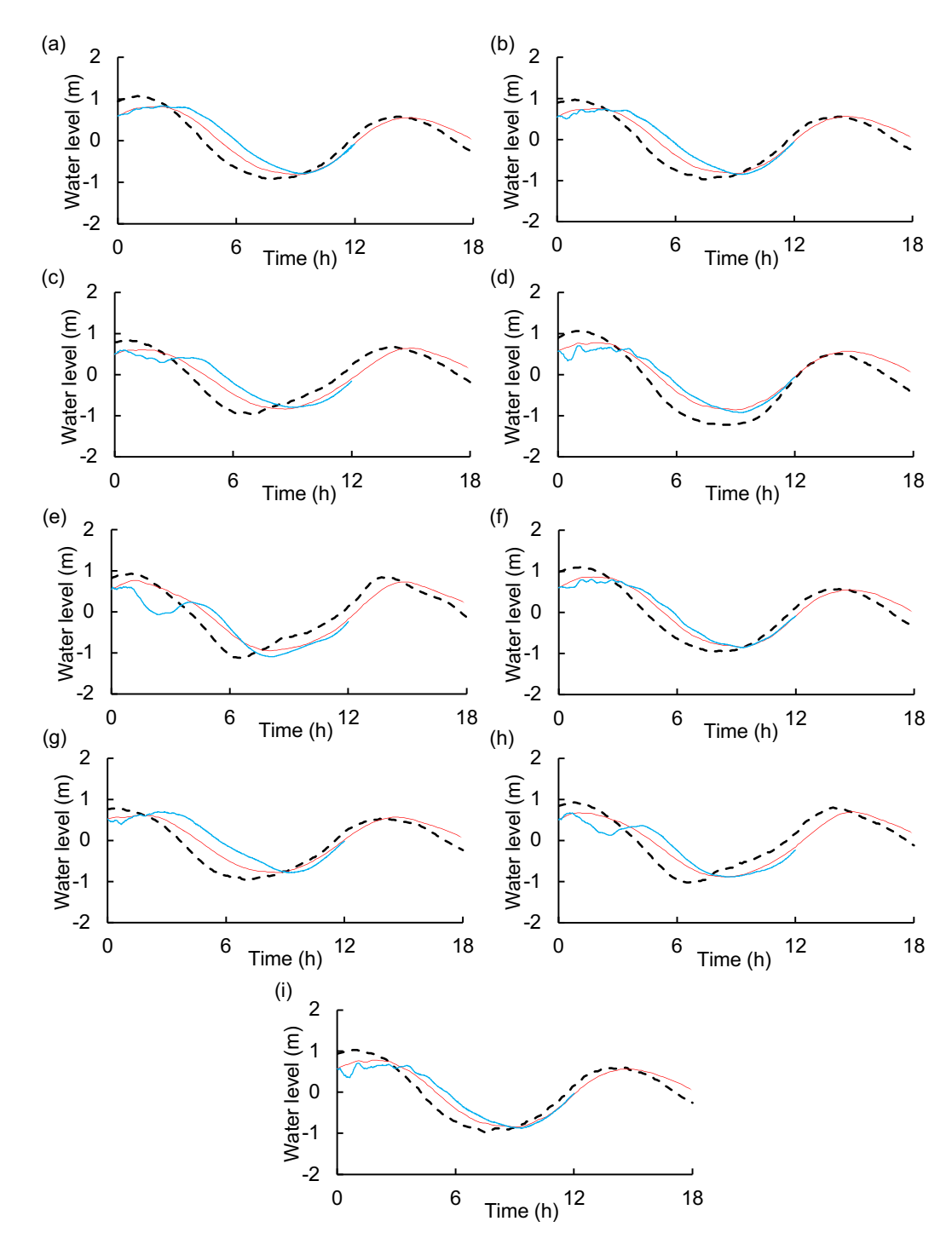


Figure 4: The comparison of calculated and observed time series of water level from 0:00 to 18:00 on 27 December 2001. The results on (a) RL, (b) BK, (c) CH, (d) LC, (e) SE, (f) SS, (g) TM, (h) UB, and (i) WC are shown. The black dashed line represents the observed results, while the red and blue lines show the calculated results using the tracks of the tropical cyclone Vamei from JMA and JTWC.





255

260

265

4.2 Storm surge induced by the 2001 Tropical Cyclone Vamei

We showed the distribution of maximum wind speed, significant wave height, and water level in computational domains 1 and 3 in case 1 (Fig. 5). The maximum wind speed is 25 m/s in domain 1. The same value was calculated in Domain 1 because the path of Tropical Cyclone Vamei is close to Singapore Island (Fig. 1). The maximum significant wave height is 5.86 m in Domain 1, while it was 4.3 m in Domain 3. The maximum significant wave height in domain 1 was calculated in southern Singapore because waves penetrated from the southeastward of Singapore, which faces the Pacific Ocean. On the other hand, the maximum water level was calculated in the north of Singapore, where its position is close to the path of Tropical Cyclone Vamei (Fig. 1). In case 1, the southern part of the tropical cyclone struck Singapore. The direction of the tropical cyclone's wind is counterclockwise in the northern hemisphere. Thus, storm surges propagated from west to east in case 1. The calculated inundation area in Singapore in case 1 is 8.06 km². In case 1, inundation occurred, especially west of Tekong Island (Fig. 5f).

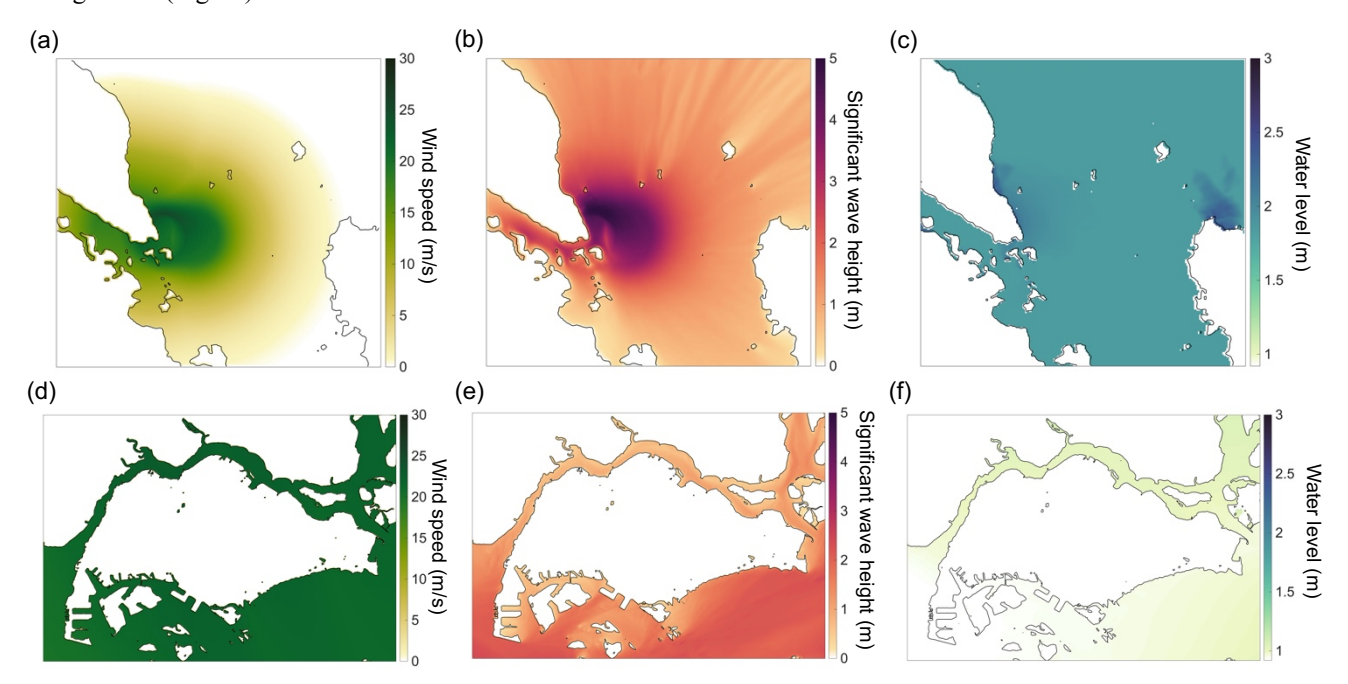


Figure 5: Calculated maximum values for the observed Tropical Cyclone Vamei simulation (Case 1). Panels (a), (b), and (c) show the maximum wind speed, significant wave height, and water levels in the D1 domain, respectively. Panels (d), (e), and (f) show the same results for the D3 domain.



275

280



4.3 Characteristics of the 1000-year design tropical cyclone

The estimated cumulative probability and annual exceedance probability versus the maximum wind speed of the tropical cyclone are shown in Fig. 6. The typhoon's maximum wind speed of 1000-year probability of occurrence is 84 knots, which can be classified as a category 2 tropical cyclone. Using the collocated JMA dataset, the relationship between maximum wind speed and minimum central pressure of tropical cyclones in the region of 0-15°N latitude and 100-125°E longitude was established (Fig. 7). The central pressure of the tropical cyclone corresponds to 949 hPa using the relation shown in Fig. 7. Based on the relation proposed by Quiring et al. (2011), the radius of maximum winds of Typhoon Vamei was 76.4 km. The radius of maximum winds of a 1000-year typhoon is 54.7 km.

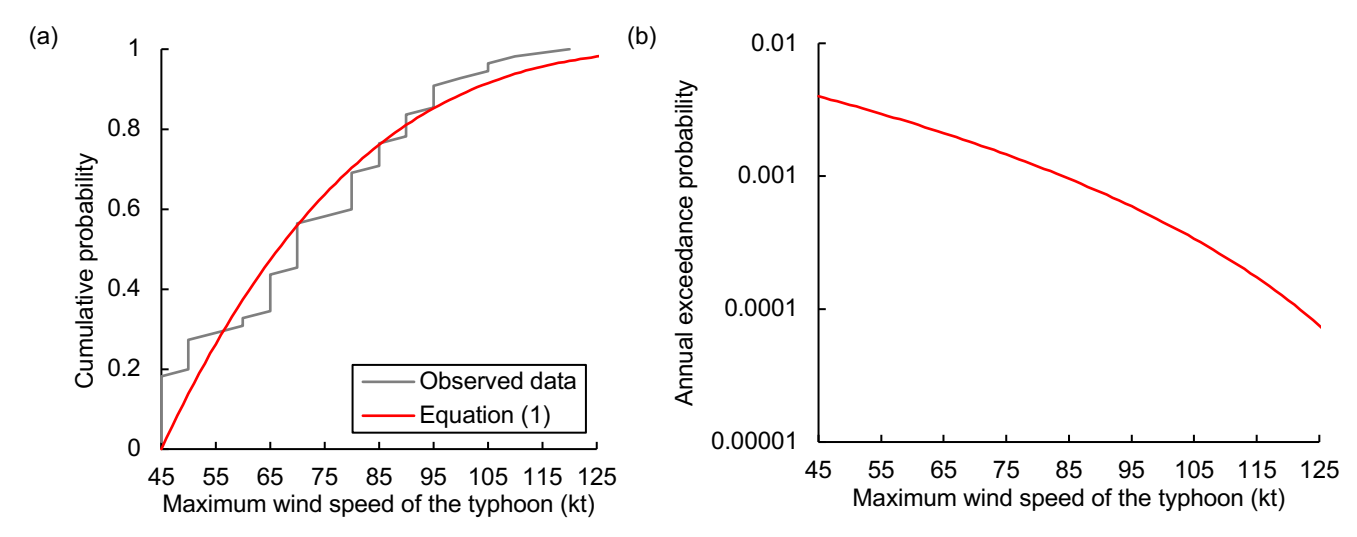


Figure 6: (a) Cumulative probability distribution for the maximum wind speed of the cyclone calculated in this study. (b) The estimated annual exceedance probability versus the maximum wind speed of the cyclone.

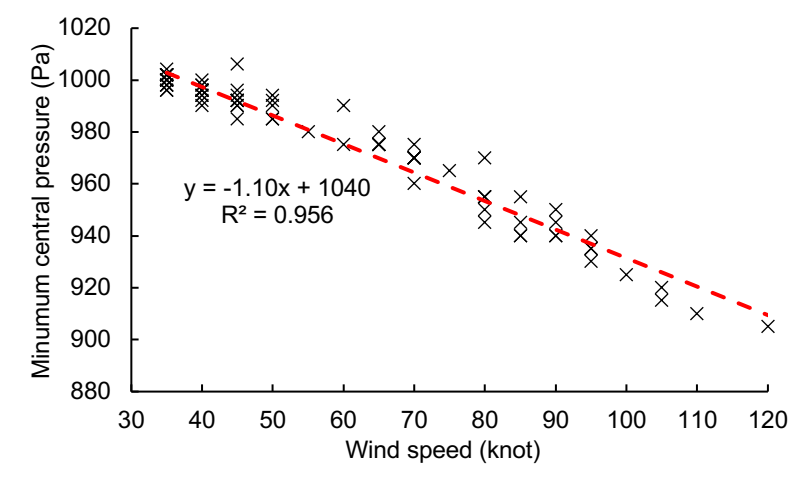


Figure 7: The relationship of minimum central pressure and maximum wind speed of the observed tropical cyclone data in the region of 0-15°N latitude and 100-125°E longitude during 1997–2023.



285



4.4 Proposed scenarios

When we shifted the tropical cyclone's path more than 0.8 degrees southward in case 5, the maximum storm surge was calculated at the northeast of Singapore Island (Fig. 8). In case 5, the northern part of the tropical cyclone strikes Singapore. The direction of the tropical cyclone's wind is counterclockwise in the northern hemisphere; thus, storm surges propagate from east to west. In this scenario, the maximum inundation area is calculated to be 8.83 km², based on the intensity of tropical cyclone Vamei, without accounting for sea level rise (Table 2).

When the 1000-year probability of occurrence was assumed, the maximum storm surge height around Singapore increased from 0.127 m to 0.595 m in Case 7 compared to Case 1 (Table 2). The inundation area increased from 8.06 km² to 10.1 km² in Case 7 compared to Case 1 (Table 2). When a 1000-year probability of occurrence was assumed, the maximum storm surge (1.34 m) was calculated when its moving path shifted 1.0° southward in Case 12 (Table 2). At the same time, the maximum inundation area was calculated when its moving path shifted 0.8° southward in Case 11 (Table 2). When a sea level rise of 0.7 m was expected, the maximum storm surge height reached 0.135 m for the size of tropical cyclone Vamei (Case 13) and 0.578 m for Vamei cyclone with a 1000-year return period (Case 15). In these cases, when the tropical cyclone path was shifted 0.8° southward, the maximum inundation areas were 19.9 km² (Case 14) and 34.5 km² (Case 16), respectively (Table 2). When the sea level rise of 2.0 m was assumed, the maximum storm surge heights were 0.133 m and 0.503 m when the size of tropical cyclone Vamei (Case 17) and 1000-year tropical cyclone (Case 19) were assumed, respectively. In these cases, when the path of the tropical cyclone was shifted 0.8° (Cases 18, 20), the maximum inundation areas were 54.1 km² and 90.7 km², respectively (Table 2).





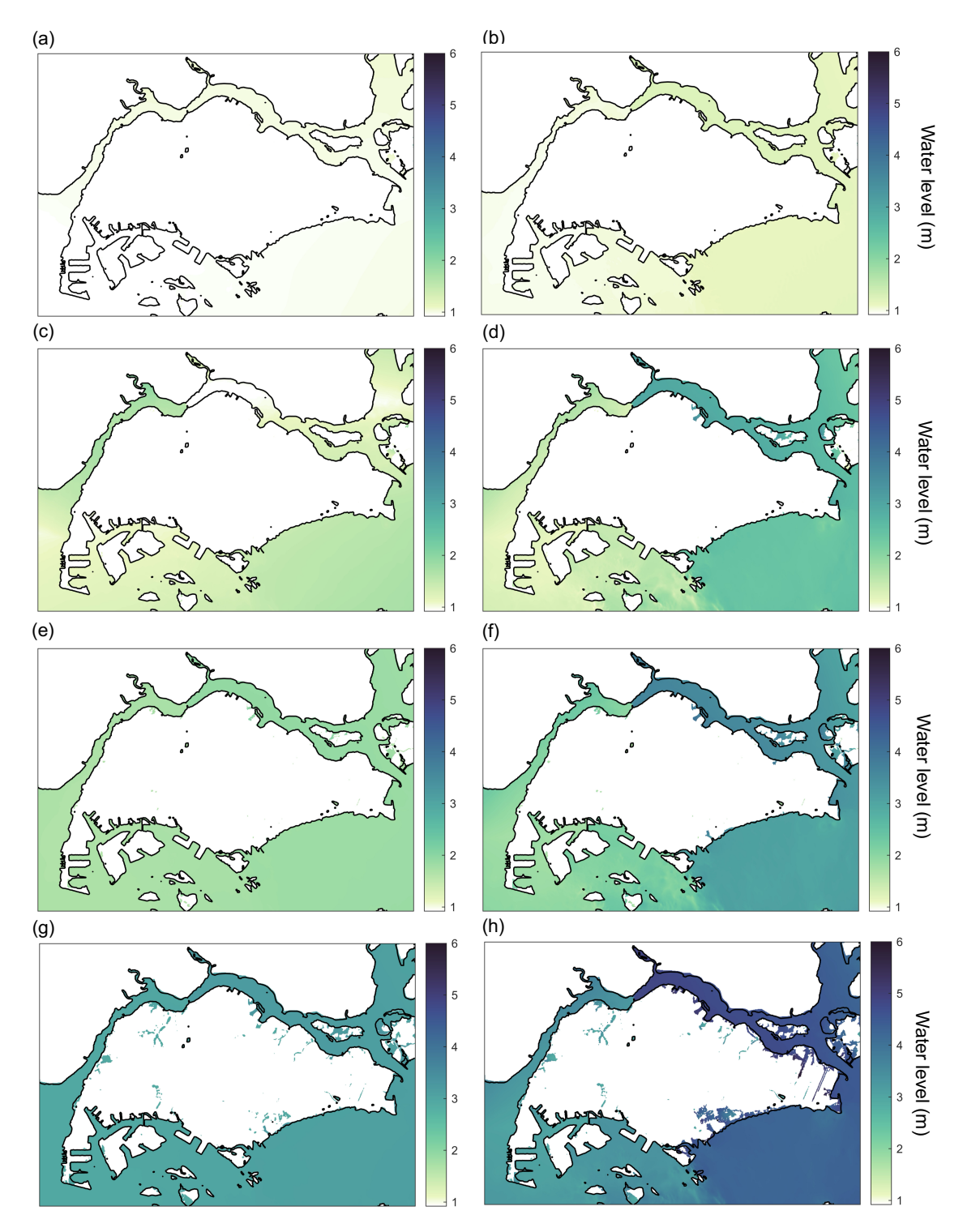


Figure 8: The calculated maximum water levels in the computational domain in D3 in (a) Case 1, (b) Case 5, (c) Case 7, (d) Case 11, (e) Case 14, (f) Case 16, (g) Case 18, and (h) Case 20.





5 Discussion

305

310

325

330

335

5.1 Equatorial cyclones

Cyclones, formidable atmospheric disturbances characterised by rotating winds and intense precipitation, owe much of their existence to the Coriolis force, a fundamental consequence of Earth's rotation (Li et al., 2012; Deng et al., 2018). This force imparts a deflection to moving objects, diverting them to the right in the Northern Hemisphere and to the left in the Southern Hemisphere (Person, 2005). Such deflection is integral to the genesis and organisation of cyclones, facilitating the establishment of their characteristic rotation and aiding in their intensification. However, in proximity to the equator, where the Coriolis force diminishes significantly, the genesis of cyclones is notably suppressed (Chang et al., 2003; Steenkamp et al., 2019).

Instead, equatorial regions are more inclined to experience phenomena such as the intertropical convergence zone (ITCZ), where converging trade winds engender a zone of low pressure and copious precipitation (Liao et al., 2023). Nevertheless, despite the infrequency of cyclonic events near the equator, exceptional circumstances such as Tropical Cyclone Vamei may sporadically occur, albeit as rare anomalies (Grey, 1968; Anthes, 1982; McBride, 1995; Chang et al., 2003; Steenkamp et al., 2019). Such occurrences underscore the multifaceted atmospheric dynamics governing tropical cyclone formation and, given the backdrop of climate change-induced alterations in global meteorological regimes, suggest a need to elucidate the ramifications of shifting atmospheric and oceanic conditions on the spatial distribution, frequency, and intensity of cyclones, including their manifestation near the equatorial latitudes.

5.2 Risk of coastal flooding in Singapore

In our simulations, the maximum storm surge was calculated in eastern Singapore. Its value was 0.127 m when the actual path and intensity of the 2001 Tropical Cyclone Vamei were assumed in case 1 (Table 2). During the storm surge on 22 December 1999, the maximum water level at tide gauge point SB (Fig. 1b) was 0.8 m (Luu et al., 1999). This storm surge was generated during king tides, so inundation occurred in Singapore (Tkalich et al., 2013). This positive anomaly of water level around Singapore is associated with intensified winds during the NE monsoon (Tkalich et al., 2013). Therefore, a sea level anomaly of the same size as Tropical Cyclone Vamei occurred in Singapore, aside from tropical cyclones. However, in this study, even when sea level rises were assumed, maximum water levels around Singapore remained the same (Table 2). This contrasts with studies showing that sea level rise can amplify coastal hazards, such as Li et al. (2018), who found that a 0.5 m sea level rise magnified tsunami flooding in Macau. In the case of our simulation, the intensity of storm surges around Singapore did not significantly change, so even if sea level rise were generated in the future, the intensity of storm surges would not significantly increase around Singapore. This means that the increase in the inundation area in Singapore in Cases 13-20 is due to sea level rise.

https://doi.org/10.5194/egusphere-2025-5703 Preprint. Discussion started: 25 November 2025

© Author(s) 2025. CC BY 4.0 License.



340



Therefore, to predict the inundation of seawater in Singapore, investigating future sea levels around Singapore is still important, and it remains an active area of research (e.g., Shaw et al., 2023; Ng et al., 2025). In addition, tsunami hazards driven by air-pressure changes during volcanic eruptions have been examined for the region, showing that the resulting water-level variations are minimal—around 1 cm in maximum (Verolino et al., 2025a, b). Understanding future sea-level changes is thus fundamental to evaluating seawater-inundation risks for Singapore.

5.3 Future risk of storm surge hazard near the Equator

Tropical cyclones generated near the equator have been reported at other locations. Indeed, 231 cyclones (or 1.74% of the total) are listed as forming within 5° of the Equator during 1848–2019 (Kilroy et al., 2020). Therefore, the risk of storm surge disasters should be investigated in the coastal areas near the equator for future climate change, meaning that the future risks of tropical cyclone generation should be investigated based on numerical simulation as some studies have been conducted (e.g., Chambers and Li, 2007; Juneng et al., 2010; Yi and Zhang, 2010; Kilroy et al., 2020).

It has been considered that Tropical cyclone Vamei was created because of a quasi-stationary low-level cyclonic circulation near Brunei called the Borneo vortex and a persistent cold surge developed rapidly over the South China Sea that happened during the northern hemisphere winter monsoon (Chang et al., 2003). The Borneo vortex is maintained by the shear vorticity and convergence that result from the interaction between the northeast monsoon winds and the mountainous Borneo terrain (Cheang, 1977; Chen et al., 1986; Johnson and Houze, 1987). It has been estimated that the intensity of the Borneo Vortex will intensify, and its frequency will decrease with future climate change (Liang et al., 2023). Thus, if a tropical cyclone were created by the Borneo vortex again, the tropical cyclone intensity might be larger than that of the 2001 Tropical Cyclone Vamei. Therefore, investigating the future size and frequency of Vamei-like tropical cyclones is necessary to reveal the future risk of storm surge hazards, especially around Singapore.

360 6 Conclusion

Storm surge hazard around the equator is rarely investigated because it has been considered that the probability of tropical cyclones is negligible. However, in December 2001, tropical cyclone Vamei developed southeast of Singapore, crossed the equator, and made landfall in Malaysia northeast of Singapore. This caused a localised storm surge, demonstrating a potential risk of cyclone-induced storm surges in the region.

365



370

375

380

385



We investigated the storm surge size caused by the 2001 Tropical Cyclone Vamei and explored potential surges had the tropical cyclone taken slightly different paths or been of a different size. The calculated maximum water levels of the storm surge caused by Tropical Cyclone Vamei were consistent with the observed maximum water levels from tide gauge data around Singapore Island. When the path of Vamei is moved southward, the maximum storm surge height around Singapore increases from 0.127 m to 0.183 m, and inundation increases from 8.06 km² to 8.83 km². When a 1000-year tropical cyclone was assumed, the maximum storm surge height increased to 0.595 m. When the sea level rise of +0.7 m and +2.0 m were assumed, the inundation area in Singapore was 34.5 km² and 90.7 km² when the path of the tropical cyclone was shifted 0.8° southward, and a 1000-year tropical cyclone was assumed. The intensity of the calculated storm surge height remained nearly the same when future sea level rise was considered; however, the inundation area in Singapore has increased. Thus, sea level rise plays an important role in expanding the inundation area, indicating that investigating future sea levels is essential for predicting seawater inundation in Singapore.

In the future, stronger tropical cyclones than Tropical Cyclone Vamei could occur due to the intensification of the Borneo vortex by future climate change. Therefore, the likelihood of changes in the frequency and intensity of tropical cyclones that may strike Singapore under future climate scenarios should be further investigated.

Appendix 1. Model calibration

We compared calculated and observed time series of water levels at the RL tide observation point, located mostly offshore from Singapore Island (Fig. A1). From 24 December to 25 December, the water level and its phases differed from the observation results. This is because the tidal current is not still distributed in the numerical domain. From 25 December to 28 December, the calculated phase of water levels is consistent with the observed ones. After that we changed the amplitude of the input tidal current, the calculated time series of water level was consistent with measured values (Fig. A1).





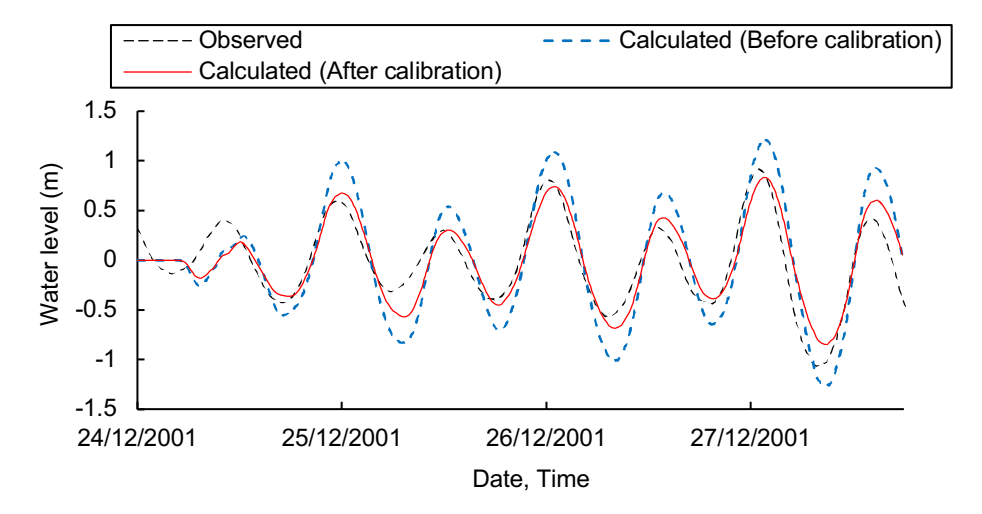


Figure A1: Time series of observed and calculated water levels before and after the calibration of the tide at RL. The location of RL is shown in Fig. 1.

Code availability

390

400

Delft-3D is the open-source code, and this code is available from https://oss.deltares.nl/web/delft3d.

Data availability

395 Tropical cyclone data used in this study are available from jma.go.jp/bosai/map.html#contents=typhoon&lang=en.

Author contribution

MW performed all analyses, created the figures, and drafted the paper. ADS provided direction for the conceptualisation. CTC, JYP, and ET created bathymetry and topography data and collected observational data. TAS and DL advised on the paper's structure and provided the general direction of the paper. ELWA investigated future typhoon size and supported its data collection.

Competing interests

The contact author has declared that none of the authors has any competing interests.





Disclaimer

Publisher's note: Copernicus Publications remains neutral with regard to jurisdictional claims made in the text, published maps, institutional affiliations, or any other geographical representation in this paper. While Copernicus Publications makes every effort to include appropriate place names, the final responsibility lies with the authors.

Acknowledgments

The tide gauge data are provided by the Maritime Port Authority (MPA). The colour maps are from the cmocean package 410 (Thyng et al., 2016).

Financial support

This Research/Project is supported by the National Research Foundation, Singapore, and the National Environment Agency, Singapore, under the National Sea Level Programme Funding Initiative (Award No. USS-IF-2020-2) and Singapore Ministry of Education Academic Research Fund MOE2019-T3-1-004. This work comprises EOS contribution number 586.

415 References

- Anthes, R. A.: *Tropical Cyclones: Their Evolution, Structure and Effects*, American Meteorological Society, Boston, 208 pp, https://doi.org/10.1007/978-1-935704-28-7, 1982.
- Bastidas, L. A., Knighton, J., and Kline, S. W.: Parameter sensitivity and uncertainty analysis for a storm surge and wave model, *Nat. Hazards Earth Syst. Sci.*, 16, 2195–2210, https://doi.org/10.5194/nhess-16-2195-2016, 2016.
- Bricker, J. D., Takagi, H., Mas, E., Sure, B., Adriano, C., Yi, C., and Roeber, V.: Spatial variation of damage due to storm surge and waves during Typhoon Haiyan in the Philippines, *J. Jpn. Soc. Civil Eng. Ser. B2*, 70(2), I_231–I_235, https://doi.org/10.2208/kaigan.70.I_231, 2014.
 - Cannaby, H., Palmer, M. D., Howard, T., Bricheno, L., Calvert, D., Krijnen, J., Wood, R., Tinker, J., Bunney, C., Harle, J., Saulter, A., O'Neill, C., Bellingham, C., and Lowe, J.: Projected sea level rise and changes in extreme storm surge and wave
- events during the 21st century in the region of Singapore, *Ocean Sci.*, 12, 613–632, https://doi.org/10.5194/os-12-613-2016, 2016.
 - CCRS (The Centre for Climate Research Singapore): *V3 Climate Projections*, available at: https://www.mss-int.sg/v3-climate-projections (accessed 13 Mar 2024), undated.
- Chambers, C. R. S. and Li, T.: Simulation of formation of a near-equatorial Typhoon Vamei (2001), *Meteorol. Atmos. Phys.*, 430 98, 67–80, https://doi.org/10.1007/s00703-006-0229-0, 2007.



435

1977.



- Chang, C.-P., Liu, C.-H., and Kuo, H.-C.: Typhoon Vamei: An equatorial tropical cyclone formation, *Geophys. Res. Lett.*, 30, 1150, https://doi.org/10.1029/2002GL016365, 2003.
- Cheang, B. K.: Synoptic feature and structure of some equatorial vortices over the South China Sea in the Malaysian region during the winter monsoon of December 1973, *Pure Appl. Geophys.*, 115, 1303–1333, https://doi.org/10.1007/BF00876181,
- Chen, G. T. J., Gerish, T. E., and Chang, C.-P.: Structure variations of the synoptic-scale cyclonic disturbances near Borneo during the WMONEX period, *Pap. Meteorol. Res.*, 9, 117–135, 2001.
- Chen, M., Murali, K., Khoo, B.-C., Lou, J., and Kumar, K.: Circulation modelling in the Strait of Singapore, *J. Coast. Res.*, 21(5), 960–972, https://doi.org/10.2112/03-0064.1, 2005.
- 440 Coles, S.: *An Introduction to Statistical Modeling of Extreme Values*, Springer, Heidelberg, 208 pp. https://doi.org/10.1007/978-1-4471-3675-0, 2001.
 - Dasgupta, S., Laplante, B., Murray, S., and Wheeler, D.: Exposure of developing countries to sea-level rise and storm surges, *Clim. Change*, 106, 567–579, https://doi.org/10.1007/s10584-010-9959-6, 2011.
 - Deltares: User Manual Delft3D-FLOW, Version 3.15.18392, Deltares, Delft, 2011.
- Deng, L., Li, T., Bi, M., Liu, J., and Peng, M.: Dependence of tropical cyclone development on Coriolis parameter: A theoretical model, *Dyn. Atmos. Oceans*, 81, 51–62, https://doi.org/10.1016/j.dynatmoce.2018.02.001, 2018.
 - Fong, L. S., Leng, M. J., and Taylor, D.: A century of anthropogenic environmental change in tropical Asia: Multi-proxy palaeolimnological evidence from Singapore's Central Catchment, *Holocene*, 30, 162–177, https://doi.org/10.1177/0959683619875819, 2020.
- 450 Fujii, T. and Mitsuda, Y.: Synthesis of a stochastic typhoon model and simulation of typhoon winds, *Annu. Disaster Prev. Res. Inst., Kyoto Univ.*, 29(B-1), 229–239, 1986.
 - Gray, W. M.: Global view of the origin of tropical disturbances and storms, *Mon. Weather Rev.*, 96, 669–700, https://doi.org/10.1175/1520-0493(1968)096<0669:GVOTOO>2.0.CO;2, 1968.
- Hasan, G. M. J., van Maren, D. S., and Ooi, S. K.: Hydrodynamic modeling of Singapore's coastal waters: nesting and model accuracy, *Ocean Model.*, 97, 141–151, https://doi.org/10.1016/j.ocemod.2015.11.005, 2016.
 - Hijmans, R. and Berkeley: *Global Administrative Areas 2015 (v2.8) Boundary, Malaysia [Dataset]*, UC Berkeley, Museum of Vertebrate Zoology, available at: http://purl.stanford.edu/bd012vf3991, 2015.
 - Holland, G. J.: An analytic model of the wind and pressure profiles in hurricanes, *Mon. Weather Rev.*, 108, 1212–1218, https://doi.org/10.1175/1520-0493(1980)108<1212:AAMOTW>2.0.CO;2, 1980.
- 460 Holland, G. J.: A revised hurricane pressure–wind model, *Mon. Weather Rev.*, 136(9), 3432–3445, https://doi.org/10.1175/2008MWR2395.1, 2008.
 - Holland, G. J., Belanger, J. I., and Fritz, A.: A revised model for radial profiles of hurricane winds, *Mon. Weather Rev.*, 138(12), 4393–4401, https://doi.org/10.1175/2010MWR3317.1, 2010.





- Hosking, J. R. M.: L-moments: Analysis and estimation of distributions using linear combinations of order statistics, J. Roy.
- 465 Stat. Soc. Ser. B (Methodological), 52(1), 105–124, https://doi.org/10.1111/j.2517-6161.1990.tb01775.x, 1990.
 - Humanitarian Data Exchange: *Indonesia Subnational Administrative Boundaries [Dataset]*, OCHA Services, available at: https://data.humdata.org/dataset/cod-ab-idn, undated.
 - IOC, IHO, and BODC: Centenary Edition of the GEBCO Digital Atlas, British Oceanographic Data Centre, Liverpool, 2003.
 - JMA (Japan Meteorological Agency): Table of Typhoon Locations 2001, available at:
- 470 https://www.data.jma.go.jp/yoho/typhoon/position-table/index.html (accessed 13 Mar 2024), undated.
 - Johnson, R. H. and Houze, R. A. Jr.: Precipitating cloud systems of the Asian monsoon, in *Monsoon Meteorology*, edited by C.-P. Chang and T. N. Krishnamurti, Oxford University Press, New York, 298–353, 1987.
 - Johnson, R. H. and Chang, C.-P.: Winter vortex: a quarter-century and beyond, *Bull. Am. Meteorol. Soc.*, 88(4), S1–S4, https://doi.org/10.1175/BAMS-88-4-S1, 2007.
- 475 JTWC (Joint Typhoon Warning Center): Western North Pacific Ocean Best Track Data, available at: https://www.metoc.navy.mil/jtwc/jtwc.html?western-pacific (accessed 13 Mar 2024), undated.
 - Juneng, L., Tangang, F. T., Reason, C. J. C., Moten, S., and Hassan, W. A. W.: Simulation of tropical cyclone Vamei (2001) using the PSU/NCAR MM5 model, *Meteorol. Atmos. Phys.*, 97, 273–290, https://doi.org/10.1007/s00703-007-0259-2, 2007.
 - Kilroy, G., Smith, R. K., and Montgomery, M. T.: An idealized numerical study of tropical cyclogenesis and evolution at the
- 480 Equator, Q. J. R. Meteorol. Soc., 146, 685–699, https://doi.org/10.1002/qj.3708, 2020.
 - Kitamoto, A.: *Digital Typhoon: Typhoon Images and Information*, available at: http://agora.ex.nii.ac.jp/digital-typhoon/index.html.en (accessed 6 Jan 2023), undated.
 - Knapp, K. R., Kruk, M. C., Levinson, D. H., Diamond, H. J., and Neumann, C. J.: The International Best Track Archive for Climate Stewardship (IBTrACS): Unifying tropical cyclone best track data, *Bull. Am. Meteorol. Soc.*, 91(3), 363–376,
- 485 https://doi.org/10.1175/2009BAMS2755.1, 2010.
 - Knapp, K. R., Diamond, H. J., Kossin, J. P., Kruk, M. C., and Schreck, C. J.: International Best Track Archive for Climate Stewardship (IBTrACS) Project, Version 4, *NOAA National Centers for Environmental Information*, https://doi.org/10.25921/82ty-9e16, 2018.
- Kotani, M., Imamura, F., and Shuto, N.: Tsunami run-up simulation and damage estimation by using geographical information system, *Proc. Coastal Eng.*, 45, 356–360 (in Japanese), 1998.
 - Liang, J., Catto, J. L., Hawcroft, M. K., Tan, M. L., Hodges, K. I., and Haywood, J. M.: Borneo vortices in a warmer climate, *npj Clim. Atmos. Sci.*, 6, 1–8, https://doi.org/10.1038/s41612-023-00461-5, 2023.
 - Li, T., Ge, X., Peng, M., and Wang, W.: Dependence of tropical cyclone intensification on the Coriolis parameter, *Trop. Cyclone Res. Rev.*, 1(2), 242–253, https://doi.org/10.6057/2012TCRR02.09, 2012.
- Liao, X., Holloway, C. E., Feng, X., Liu, C., Lyu, X., Xue, Y., and Qiao, F.: Observed interannual relationship between ITCZ position and tropical cyclone frequency, *J. Climate*, 36(16), 5587–5603, https://doi.org/10.1175/JCLI-D-22-0487.1, 2023.



510



- Li, L., Switzer, A. D., Wang, Y., Chan, C. H., Qiu, Q., and Weiss, R.: A modest 0.5-m rise in sea level will double the tsunami hazard in Macau, *Sci. Adv.*, 4, eaat1180, https://doi.org/10.1126/sciadv.aat1180, 2018.
- Lin, Y. C., Jenkins, S. F., Chow, J. R., Biass, S., Woo, G., and Lallemant, D.: Modeling downward counterfactual events: Unrealized disasters and why they matter, *Front. Earth Sci.*, 8, 575048, https://doi.org/10.3389/feart.2020.575048, 2020.
 - Luu, Q. H., Tkalich, P., Choo, H. K., and Wang, B.: A storm surge forecasting system for the Singapore Strait, *Smart Water*, 1, 2, https://doi.org/10.1186/s40713-016-0002-3, 2016.
- Maritime and Port Authority of Singapore: *Towards a Future-Ready Maritime Singapore: Annual Report 2014 An Inaugural Sustainability/Integrated Report*, Maritime and Port Authority of Singapore, Singapore, 2014.
 - McBride, J. L.: Tropical cyclone formation, in *Global Perspectives on Tropical Cyclones*, edited by R. L. Elsberry, WMO/TD-No. 693, World Meteorological Organization, Geneva, 63–105, 1995.
 - McInnes, K. L., Hoeke, R. K., Walsh, K. J. E., O'Grady, J. G., and Hubbert, G. G.: Application of a synthetic cyclone method for assessment of tropical cyclone storm tides in Samoa, *Nat. Hazards*, 80, 425–444, https://doi.org/10.1007/s11069-015-1970-4, 2016.
 - Miller, B. B. and Carter, C.: The test article, *J. Sci. Res.*, 12, 135–147, https://doi.org/10.1234/56789, 2015.
 - Muñoz, D. F., Yin, D., Bakhtyar, R., Moftakhari, H., Xue, Z., Mandli, K., and Ferreira, C.: Inter-model comparison of Delft3D-FM and 2D HEC-RAS for total water level prediction in coastal to inland transition zones, *J. Am. Water Resour. Assoc.*, 58, e12952, https://doi.org/10.1111/1752-1688.12952, 2022.
- Navionics: *Navionics ChartViewer*, available at: https://webapp.navionics.com/ (accessed 13 Mar 2024), 2023.

 Neumann, J. E., Emanuel, K., Ravela, S., Ludwig, L., Kirshen, P., Bosma, K., and Martinich, J.: Joint effects of storm surge and sea-level rise on U.S. coasts: new economic estimates of impacts, adaptation, and benefits of mitigation policy, *Clim. Change*, 129, 337–349, https://doi.org/10.1007/s10584-014-1304-z, 2015.
- Ng, T., Garner, G. G., Weeks, J. H., Hogarth, P., Palmer, M. D., Li, T., Moise, A., and Horton, B. P.: Robust sea-level projections for Singapore by 2100 and 2150, *J. Geophys. Res.: Oceans*, 130, e2024JC021840, https://doi.org/10.1029/2024JC021840, 2025.
 - Persson, A.: The Coriolis effect, *Hist. Meteorol.*, 2, 1–24, 2005.
 - Puah, J. Y., Haigh, I. D., Lallemant, D., Morgan, K., Peng, D., Watanabe, M., and Switzer, A. D.: Importance of tides and winds in influencing the nonstationary behaviour of coastal currents in offshore Singapore, *Ocean Sci.*, 20(5), 1229–1246,
- 525 https://doi.org/10.5194/os-20-1229-2024, 2024.
 - Quiring, S. M., Schumacher, A. B., Labosier, C. F., and Zhu, L.: Variations in mean annual tropical cyclone size in the Atlantic, *J. Geophys. Res.*, 116, D09114, https://doi.org/10.1029/2010JD015011, 2011.
 - Shaw, T. A., Li, T., Ng, T., Cahill, N., Chua, S., Majewski, J. M., Nathan, Y., Garner, G. G., Kopp, R. E., Hanebuth, T. J. J., Switzer, A. D., and Horton, B. P.: Deglacial perspectives of future sea level for Singapore, *Commun. Earth Environ.*, 4, 204,
- 530 https://doi.org/10.1038/s43247-023-00835-9, 2023.



560



- Singapore Land Authority: 10-Meter Digital Terrain Model (DTM) Map of Singapore (2019 Version) [Dataset], Singapore Land Authority, Singapore, 2019.
- Steenkamp, S. C., Kilroy, G., and Smith, R. K.: Tropical cyclogenesis at and near the Equator, Q. J. R. Meteorol. Soc., 145(722), 1846–1864, https://doi.org/10.1002/qj.3519, 2019.
- 535 SwissRe: *Industry-First Global Storm Surge Zones*, available at: https://www.swissre.com/dam/jcr:dedf399f-af17-4061-928f-dba8229c1499/industry-first-global-storm-surge-zones.pdf (accessed 13 Mar 2024), 2017.
 - Switzer, A. D., Christensen, J., Aldridge, J., Taylor, D., Churchill, J., Watson, H., Fraser, M. W., and Sandhaw, J.: The utility of historical records for hazard analysis in an area of marginal cyclone influence, *Commun. Earth Environ.*, 4, 193, https://doi.org/10.1038/s43247-023-00831-z, 2023.
- Tadesse, M., Wahl, T., and Cid, A.: Data-driven modeling of global storm surges, *Front. Mar. Sci.*, 7, 563537, https://doi.org/10.3389/fmars.2020.563537, 2020.
 - Thyng, K., Greene, C., Hetland, R., Zimmerle, H., and DiMarco, S.: True Colors of Oceanography: Guidelines for Effective and Accurate Colormap Selection, Oceanography, 29, 9–13, https://doi.org/10.5670/oceanog.2016.66, 2016.
- Tkalich, P., Vethamony, P., Babu, M. T., and Malanotte-Rizzoli, P.: Surges in the Singapore Strait due to winds in the South China Sea, *Nat. Hazards*, 66, 1345–1362, https://doi.org/10.1007/s11069-012-0223-5, 2013a.
 - Tkalich, P., Vethamony, P., Luu, Q. H., and Babu, M. T.: Sea level trend and variability in the Singapore Strait, *Ocean Sci.*, 9, 293–300, https://doi.org/10.5194/os-9-293-2013, 2013b.
 - Tun, K. P. P.: Optimisation of Reef Survey Methods and Application of Reef Metrics and Biocriteria for the Monitoring of Sediment Impacted Reefs, PhD Thesis, National University of Singapore, 179 pp, 2012.
- 550 TPXO: *The OSU TOPEX/POSEIDON Global Inverse Solution*, available at: http://volkov.oce.orst.edu/tides/global.html (accessed 13 Mar 2024), 2014.
 - Urban Redevelopment Authority: *Master Plan 2019 Region Boundary (No Sea) (KML) [Dataset]*, Open Government Products, available at: https://beta.data.gov.sg/datasets/d_ef3fc5c7a62139471ebc9ffa598b60e8/view (accessed 13 Mar 2024), 2019.
- Verolino, A., Watanabe, M., Felix, R., Elaine, T., Yang, J., Weiss, R., Lynett, P., and Switzer, A.: Forced and free waves of simulated volcanic meteo-tsunamis in the South China Sea, *npj Nat. Hazards*, 2(1), 1–9, https://doi.org/10.1038/s44304-025-00001-2, 2025a.
 - Verolino, A., Watanabe, M., Felix, R., Conway, E. C., and Switzer, A.: An initial assessment of volcanic meteo-tsunami hazard in the South China Sea: What we learned and how to move forward, *Georisk: Assess. Manag. Risk Eng. Syst. Geohazards*, 1–21, https://doi.org/10.1080/17499518.2025.1234567, 2025b.
 - Wada, A., Usui, N., and Sato, K.: Relationship of maximum tropical cyclone intensity to sea surface temperature and tropical cyclone heat potential in the North Pacific Ocean, *J. Geophys. Res.*, 117, D11118, https://doi.org/10.1029/2012JD017583, 2012.





- Wang, T., Belle, I., and Hassler, U.: Modelling of Singapore's topographic transformation based on DEMs, *Geomorphology*, 231, 365–375, https://doi.org/10.1016/j.geomorph.2014.11.033, 2015.
 - Wang, P., Wang, C., Gou, Y., et al.: Future changes and uncertainty in tropical cyclone genesis over the western North Pacific: insights from the dynamic genesis potential index using CMIP6 models, *Clim. Dyn.*, 63, 99, https://doi.org/10.1007/s00382-025-07599-7, 2025.
- Watanabe, M., Bricker, J. D., Goto, K., and Imamura, F.: Factors responsible for the limited inland extent of sand deposits on Leyte Island during 2013 Typhoon Haiyan, *J. Geophys. Res.: Oceans*, 122(4), 2795–2812, https://doi.org/10.1002/2016JC012361, 2017.
 - Watanabe, M., Goto, K., Bricker, J. D., and Imamura, F.: Are inundation limit and maximum extent of sand useful for differentiating tsunamis and storms? An example from sediment transport simulations on the Sendai Plain, Japan, *Sediment. Geol.*, 364, 204–216, https://doi.org/10.1016/j.sedgeo.2017.11.003, 2018.
- Widana Arachchige, E. L., Zhou, W., Toumi, R., and others: Projected tropical cyclone genesis and seasonality changes in the Northern Hemisphere under a warming climate, *npj Clim. Atmos. Sci.*, 8, 288, https://doi.org/10.1038/s41612-025-00821-3, 2025.
 - Woo, G.: Counterfactual disaster risk analysis, *Variance*, 10, 279–291, https://doi.org/10.1016/S2542-5196(18)30209-2, 2016.
- 580 Woo, G.: Downward counterfactual search for extreme events, *Front. Earth Sci.*, 7, 260, https://doi.org/10.3389/feart.2019.00260, 2019.
 - Yi, B. Q. and Zhang, Q. H.: Near-equatorial typhoon development: Climatology and numerical simulations, *Adv. Atmos. Sci.*, 27(5), 1014–1024, https://doi.org/10.1007/s00376-010-9191-8, 2010.